

THE INTERACTION BETWEEN LINE FORCE ARRAYS AND PLANAR CRACKS

J. P. HIRTH

Metallurgical Engineering Department, The Ohio State University,
Columbus, Ohio 43210, U.S.A.

and

R. G. HOAGLAND and P. C. GEHLEN

Metal Science Group, Battelle, Columbus Laboratories, Columbus, Ohio 43201, U.S.A.

(Received 30 August, 1973; revised 29 January 1974)

Abstract—The utility of line force fields in computer simulations of lattice defects is discussed. These fields are shown to provide a facile method for introducing realistic flexible boundary conditions on simulated atomic crystallites. The pertinent elastic fields for line force arrays lying parallel to the tip of a planar crack are presented.

1. INTRODUCTION

In recent years there has been a growing interest in the computer simulation of a planar crack progressing through a discrete atomic crystallite[1-4]. There has been a parallel development in the study of straight dislocations in discrete crystallites[5-7]. The essence of these treatments[7] is to divide the crystallite into three regions: region I which surrounds the dislocation line or crack tip and is comprised of discrete atoms, region II which completely surrounds region I and is considered to be an elastic continuum with virtual atomic sites imbedded in it, and region III which surrounds region II and is an elastic continuum.

Early computer models imposed so-called rigid boundary conditions on the boundary between regions I and II; that is to say, that the atoms in region II were held fixed in the positions given by the linear elastic model of the defect being simulated. Since rigid boundaries do not allow for volume changes that are experimentally known to occur around defects, it soon became apparent that this type of boundary imposed extraneous stress fields on atoms in region I, resulting in excessively large computed Peierls stresses[8] and fracture stresses[2].

These difficulties were circumvented in later models[3-7] with flexible boundary conditions permitting displacements produced by the nonlinear elastic field of the atomic force law governing the discrete atomic interactions and allowing compatible equilibration of forces and displacements at the boundary. The use of flexible boundary conditions produced marked changes in the properties of the simulated entities; for example, changing dislocation mobilities by orders of magnitude[8].

The flexible boundary methods described in[7], have been found to be most expedient and accurate in treating dislocation problems. In this scheme, atomic relaxation in region I is performed with its boundary constrained, net forces acting on atoms at the boundary are

calculated, and displacements associated with such line forces are imposed on all three regions using a Green's function formalism derived by Hirth[9]. The process is iterated until equilibrium is approached asymptotically. Also, the dislocation calculations have shown that the flexible boundary method produces marked changes in defect configuration from the result with rigid boundaries whether anisotropic or isotropic elasticity is used to describe the line force displacement fields, but that the difference between the anisotropic and isotropic cases is only a few percent[6, 7].

In view of the above discussion, and particularly in light of the fact that in[4] the wrong cleavage plane was predicted for α -iron, the extension of the flexible boundary methodology to the crack problem is of interest. Although the effect of the image forces required to make the crack faces stress free can, in principle, be handled numerically, our experience has shown that convergence problems arise because the crack length dealt with in the computer is too small. Therefore, it is desirable to have the linear elastic solution to the displacement fields of line forces in the presence of a crack.

In principle, the anisotropic elastic solution can be obtained for this problem. Indeed, the anisotropic solution for a dislocation in the presence of a planar crack has been presented[10]; however, except for special symmetry directions of the dislocation line, the solution involves the numerical solution of a sixth order secular equation and then a line integral for the field at each point of the medium. Since the isotropic result was found to give a fairly accurate approximation of the anisotropic result in the dislocation case, and because the isotropic case can be solved analytically, we present the isotropic result here.

The problem of primary interest is the field of a single line force in the presence of a crack semi-infinite in length. However, we also present the result for the case of line force couples without moment. The semi-infinite crack case is selected because it is the one relevant to atomic simulations, i.e. near tip elastic fields are of primary importance. The nonlinear field of a dislocation can be represented in terms of the latter defect[6, 7], so the result for its field may be useful in treating the plastic relaxation at a crack tip by dislocation motion.

1.1 Computational method

All cases of interest in the present work are two-dimensional elasticity problems. The appropriate geometry for the problems is depicted in Fig. 1. The forces are uniformly distributed along a line parallel to x_3 with the crack plane normal to x_2 . The solution for

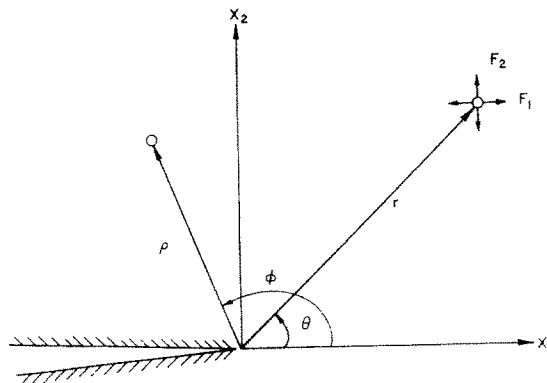


Fig. 1. Geometry for a planar crack interacting with line forces at r . Displacements are evaluated at p . The crack tip is at the origin. Both the crack tip and the line forces are parallel to x_3 .

this type of problem can be obtained by the method of Rice[11] and Muskhelishvili[12]. The pertinent representation in the complex plane is given in Fig. 2. The elastic interaction field between the line forces and the crack in the plane stress and plane strain cases[11] (i.e. the additional displacements produced by creating a crack in an otherwise homogeneous solid) can be expressed in terms of a function $\phi(z)$ and its derivatives with respect to z , ϕ' and ϕ'' , as follows[13]. The displacements are

$$u_1 + iu_2 = [\kappa\phi(z) - \phi(\bar{z}) - (z - \bar{z})\overline{\phi'(z)}]/2\mu$$

where μ is the shear modulus, $\kappa = 3 - 4\nu$ for plane strain and $\kappa = (3 - \nu)/(1 + \nu)$ for plane stress, with ν Poisson's ratio. A bar over a quantity has the usual meaning of complex conjugate. The stresses are

$$\begin{aligned} \sigma_{22} - i\sigma_{12} &= \phi'(z) + \phi'(\bar{z}) + (z - \bar{z})\overline{\phi''(z)} \\ \sigma_{11} &= 4 \operatorname{Re}[\phi'(z)] - \sigma_{22} \\ \sigma_{33} &= \nu(\sigma_{11} + \sigma_{22}) \\ \sigma_{13} &= \sigma_{23} = 0. \end{aligned} \tag{2}$$

In the antiplane strain case[11]

$$u_3 = \operatorname{Im}[\omega(z)]/\mu \tag{3}$$

and

$$\sigma_{23} + i\sigma_{13} = \omega'(z), \quad \text{other } \sigma_{ij} = 0. \tag{4}$$

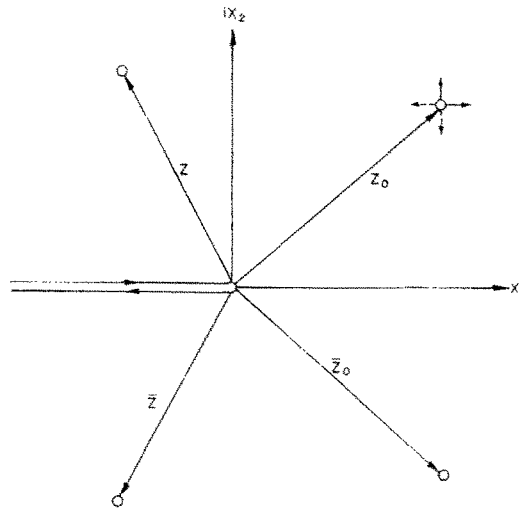


Fig. 2. Representation of Fig. 1 in the complex plane.

1.2 Single line forces

First, we consider the line forces F_1 and F_2 . Any line force acting in the x_1x_2 plane can be decomposed into components along x_1 and x_2 and expressed in terms of the above sources by superposition. For this case, contour integration of equation (91) of Rice[11], followed by integration with respect to z yields.

$$\phi(z) = L \ln(z^{1/2} + \bar{z}_0^{1/2}) + Q \ln(z^{1/2} + z_0^{1/2}) + K/\{\bar{z}_0^{1/2}(z^{1/2} + \bar{z}_0^{1/2})\} \tag{5}$$

with

$$\begin{aligned} L &= -F_1\kappa(1 + i\gamma)/2\pi(\kappa + 1) \\ Q &= F_1(1 + i\gamma)/2\pi(\kappa + 1) \\ K &= F_1 r \sin \theta(\gamma + i)/2\pi(\kappa + 1) \\ \gamma &= F_2/F_1. \end{aligned}$$

The functions $\phi'(z)$ and $\phi''(z)$ follow by differentiation and $\phi(\bar{z})$ is given by equation (5) with \bar{z} substituted for z . Explicitly, the desired displacements are

$$\begin{aligned} u_1 &= \frac{F_1\kappa}{4\pi(\kappa + 1)\mu} \left\{ \ln \rho E - \left(\frac{\kappa + \kappa^{-1}}{2} \right) \ln \rho D + \gamma(\kappa - \kappa^{-1})\eta \right. \\ &\quad + \frac{P\gamma \sin \theta}{D} \left(\cos \frac{\theta - \varphi}{2} + P \cos \theta \right) - \frac{P \sin \theta}{D} \left(\sin \frac{\theta - \varphi}{2} + P \sin \theta \right) \\ &\quad - \frac{P\gamma \sin \theta}{\kappa E} \left(\cos \frac{\theta + \varphi}{2} + P \cos \theta \right) + \frac{P \sin \theta}{\kappa E} \left(\sin \frac{\theta + \varphi}{2} + P \sin \theta \right) \\ &\quad + \frac{\gamma \sin \varphi}{D} \left(\cos \varphi + P \cos \frac{\theta - \varphi}{2} \right) - \frac{\sin \varphi}{D} \left(\sin \varphi - P \sin \frac{\theta - \varphi}{2} \right) \\ &\quad - \frac{\gamma \sin \varphi}{\kappa E} \left(\cos \varphi + P \cos \frac{\theta + \varphi}{2} \right) + \frac{\sin \varphi}{\kappa E} \left(\sin \varphi + P \sin \frac{\theta + \varphi}{2} \right) \\ &\quad + \frac{P\gamma \sin \theta \sin \varphi}{\kappa D^2} \left[\sin \frac{\theta - 3\varphi}{2} + 2P \sin (\theta - \varphi) + P^2 \sin \frac{3\theta - \varphi}{2} \right] \\ &\quad \left. + \frac{P \sin \theta \sin \varphi}{\kappa D^2} \left[\cos \frac{\theta - 3\varphi}{2} + 2P \cos (\theta - \varphi) + P^2 \cos \frac{3\theta - \varphi}{2} \right] \right\} \\ u_2 &= \frac{F_1\kappa}{4\pi(\kappa + 1)\mu} \left\{ \gamma \ln \rho E - \gamma \frac{(\kappa + \kappa^{-1})}{2} \ln \rho D - (\kappa - \kappa^{-1})\eta \right. \\ &\quad + \frac{P\gamma \sin \theta}{D} \left(\sin \frac{\theta - \varphi}{2} + P \sin \theta \right) + \frac{P \sin \theta}{D} \left(\cos \frac{\theta - \varphi}{2} + P \cos \theta \right) \\ &\quad - \frac{P\gamma \sin \theta}{\kappa E} \left(\sin \frac{\theta + \varphi}{2} + P \sin \theta \right) - \frac{P \sin \theta}{\kappa E} \left(\cos \frac{\theta + \varphi}{2} + P \cos \theta \right) \\ &\quad + \frac{\gamma \sin \varphi}{D} \left(\sin \varphi - P \sin \frac{\theta - \varphi}{2} \right) + \frac{\sin \varphi}{D} \left(\cos \varphi + P \cos \frac{\theta - \varphi}{2} \right) \\ &\quad - \frac{\gamma \sin \varphi}{\kappa E} \left(\sin \varphi + P \sin \frac{\theta + \varphi}{2} \right) - \frac{\sin \varphi}{\kappa E} \left(\cos \varphi + P \cos \frac{\theta + \varphi}{2} \right) \\ &\quad + \frac{P\gamma \sin \theta \sin \varphi}{\kappa D^2} \left[\cos \frac{\theta - 3\varphi}{2} + 2P \cos (\theta - \varphi) + P^2 \cos \frac{3\theta - \varphi}{2} \right] \\ &\quad \left. - \frac{P \sin \theta \sin \varphi}{\kappa D^2} \left[\sin \frac{\theta - 3\varphi}{2} + 2P \sin (\theta - \varphi) + P^2 \sin \frac{3\theta - \varphi}{2} \right] \right\} \end{aligned} \tag{6}$$

with

$$D = 1 + P^2 + 2P \cos \frac{\theta + \varphi}{2}$$

$$E = 1 + P^2 + 2P \cos \frac{\theta - \varphi}{2}$$

$$\eta = \tan^{-1} \frac{\sin(\varphi/2) - P \sin(\theta/2)}{\cos(\varphi/2) + P \cos(\theta/2)}$$

$$P = (r/\rho)^{1/2}$$

where r and ρ are defined in Fig. 1. The above displacements provide the Green's function to generate the displacement field of a set of forces bounding region I for a mode I or mode II crack problem. The associated stress field is not of direct interest in the computer simulation application, but can be found either by differentiation of equation (6) and use of Hooke's law or from equations (2) and (5). In the case where ϕ and θ approach π and where ρ and r are large, the stress field agrees with that found by Hetenyi and Dundurs[14] for the line forces lying parallel to the planar free surface of a semi-infinite medium.

The field of the line forces themselves, that gives the total field when added to the above interaction field, is[9]

$$u_1 = -\frac{F_1}{4\pi\mu} \left\{ \frac{\kappa + 3}{\kappa + 1} \ln \rho [1 + P^4 - 2P^2 \cos(\theta - \varphi)]^{1/2} \right.$$

$$+ \frac{1}{\kappa + 1} \frac{[2(\sin \varphi - P^2 \sin \theta)^2 - \gamma \sin 2\varphi - \gamma P^4 \sin 2\theta + 2\gamma P^2 \sin(\theta + \varphi)]}{[1 + P^4 - 2P^2 \cos(\theta - \varphi)]} \left. \right\} \tag{7}$$

$$u_2 = \frac{F_1}{4\pi\mu} \left\{ -\gamma \frac{\kappa + 3}{\kappa + 1} \ln \rho [1 + P^4 - 2P^2 \cos(\theta - \varphi)]^{1/2} \right.$$

$$+ \frac{1}{\kappa + 1} \frac{[-2\gamma(\cos \varphi - P^2 \cos \theta)^2 + \sin 2\varphi + P^4 \sin 2\theta - 2P^2 \sin(\theta + \varphi)]}{[1 + P^4 - 2P^2 \cos(\theta - \varphi)]} \left. \right\}.$$

For a line force in the x_3 -direction, of interest in mode III crack problems, the generating function is

$$\omega(z) = (i F_3/2\pi)[\ln(z^{1/2} + z_0^{1/2}) - \ln(z^{1/2} + \bar{z}_0^{1/2})] \tag{8}$$

yielding the interaction displacement field

$$u_3 = \frac{F_3}{4\pi\mu} \ln(D/E). \tag{9}$$

The field of the defect itself is[9]

$$u_3 = -\frac{F_3}{4\pi} \ln\{\rho^2 [1 + P^4 - 2P^2 \cos(\theta - \varphi)]\}. \tag{10}$$

1.3 Line force couples

In the plane strain case, the fields of line force couples without moment, also depicted in Fig. 1, are of interest since they give a representation of the nonlinear field of a dislocation and because they can be superposed to give the field of an edge dislocation itself. In this case a line force F_1 is applied at x_1, x_2 , a line force $-F_1$ is applied at $x_1 - \delta x_1, x_2$, and the limit $\delta x_1 \rightarrow 0$ is taken while keeping the moment $M_1 = F_1 \delta x_1$ constant; a similar procedure yields M_2 .

Proceeding as above, we find for the interaction field between an orthogonal pair of line force couples at r and the crack tip, the generating function

$$\begin{aligned} \phi(z) = & \frac{A}{\bar{z}_0^{1/2}(z^{1/2} + \bar{z}_0^{1/2})} - \frac{B}{z_0^{1/2}(z^{1/2} + z_0^{1/2})} \\ & + \frac{i Br \sin \theta}{\bar{z}_0^{3/2}(z^{1/2} + \bar{z}_0^{1/2})} + \frac{i Br \sin \theta}{\bar{z}_0(z^{1/2} + \bar{z}_0^{1/2})^2} \end{aligned} \quad (11)$$

with

$$\begin{aligned} A &= M_1(\kappa + \alpha\kappa - 2\alpha)/4\pi(\kappa + 1) \\ B &= M_1(1 - \alpha)/4\pi(\kappa + 1) \\ \alpha &= M_2/M_1. \end{aligned}$$

In this case the interaction displacement field is

$$\begin{aligned} u_1 = & \frac{1}{2\mu} \left\{ -\frac{(\kappa A + B)}{\rho P D} \left(\cos \frac{\theta - \varphi}{2} + P \cos \theta \right) + \frac{(A + B\kappa)}{\rho P E} \left(\cos \frac{\theta + \varphi}{2} + P \cos \theta \right) \right. \\ & + \frac{B\kappa \sin \theta}{\rho P D} \left(\sin \frac{3\theta - \varphi}{2} + P \sin 2\theta \right) + \frac{B\kappa \sin \theta}{\rho D^2} \\ & \times \left[\sin(\theta - \varphi) + 2P \sin \frac{3\theta - \varphi}{2} + P^2 \sin 2\theta \right] \\ & - \frac{B \sin \theta}{\rho P E} \left(\sin \frac{3\theta + \varphi}{2} + P \sin 2\theta \right) - \frac{B \sin \theta}{\rho E^2} \left[\sin(\theta + \varphi) + 2P \sin \frac{3\theta + \varphi}{2} + P^2 \sin 2\theta \right] \\ & - \frac{A \sin \varphi}{\rho P D^2} \left[\sin \frac{\theta - 3\varphi}{2} + 2P \sin(\theta - \varphi) + P^2 \sin \frac{3\theta - \varphi}{2} \right] \\ & - \frac{B \sin \varphi}{\rho P E^2} \left[\sin \frac{\theta + 3\varphi}{2} + 2P \sin(\theta + \varphi) + P^2 \sin \frac{3\theta + \varphi}{2} \right] \\ & - \frac{B \sin \theta \sin \varphi}{\rho P D^2} \left[\cos \frac{3\theta - 3\varphi}{2} + 2P \cos(2\theta - \varphi) + P^2 \cos \frac{5\theta - \varphi}{2} \right] \\ & \left. - \frac{2B \sin \theta \sin \varphi}{\rho D^3} \left[\cos(\theta - 2\varphi) + 3P \cos \frac{3\theta - 3\varphi}{2} + 3P^2 \cos(2\theta - \varphi) + P^3 \cos \frac{5\theta - \varphi}{2} \right] \right\} \end{aligned} \quad (12)$$

$$\begin{aligned}
 u_2 = & \frac{1}{2\mu} \left\{ -\frac{(\kappa A - B)}{\rho PD} \left(\sin \frac{\theta - \varphi}{2} + P \sin \theta \right) + \frac{(A - B\kappa)}{\rho PE} \left(\sin \frac{\theta + \varphi}{2} + P \sin \theta \right) \right. \\
 & - \frac{B\kappa \sin \theta}{\rho PD} \left(\cos \frac{3\theta - \varphi}{2} + P \cos 2\theta \right) - \frac{B\kappa \sin \theta}{\rho D^2} \\
 & \times \left[\cos(\theta - \varphi) + 2P \cos \frac{3\theta - \varphi}{2} + P^2 \cos 2\theta \right] \\
 & + \frac{B \sin \theta}{\rho PE} \left(\cos \frac{3\theta + \varphi}{2} + P \cos 2\theta \right) + \frac{B \sin \theta}{\rho E^2} \\
 & \times \left[\cos(\theta + \varphi) + 2P \cos \frac{3\theta + \varphi}{2} + P^2 \cos 2\theta \right] \\
 & - \frac{A \sin \varphi}{\rho PD^2} \left[\cos \frac{\theta - 3\varphi}{2} + 2P \cos(\theta - \varphi) + P^2 \cos \frac{3\theta - \varphi}{2} \right] \\
 & + \frac{B \sin \varphi}{\rho PE^2} \left[\cos \frac{\theta + 3\varphi}{2} + 2P \cos(\theta + \varphi) + P^2 \cos \frac{3\theta + \varphi}{2} \right] \\
 & + \frac{B \sin \theta \sin \varphi}{\rho PD^2} \left[\sin \frac{3\theta - 3\varphi}{2} + 2P \sin(2\theta - \varphi) + P^2 \sin \frac{5\theta - \varphi}{2} \right] \\
 & \left. + \frac{2B \sin \theta \sin \varphi}{\rho D^3} \left[\sin(\theta - 2\varphi) + 3P \sin \frac{3\theta - 3\varphi}{2} + 3P^2 \sin(2\theta - \varphi) + P^3 \sin \frac{5\theta - \varphi}{2} \right] \right\}.
 \end{aligned}$$

In this case the field of the defect itself is[6, 9]

$$\begin{aligned}
 u_1 = & \frac{M_1(\sin \varphi - P^2 \sin \theta)}{2\pi\mu\rho[1 + P^4 - 2P^2 \cos(\theta - \varphi)]} \\
 & \left\{ \frac{\kappa - 1}{\kappa + 1} - \frac{1 - \alpha [\cos 2\varphi + P^4 \cos 2\theta - 2P^2 \cos(\theta + \varphi)]}{\kappa + 1 [1 + P^4 - 2P^2 \cos(\theta - \varphi)]} \right\} \\
 u_2 = & \frac{M_1(\sin \varphi - P^2 \sin \theta)}{2\pi\mu\rho[1 + P^4 - 2P^2 \cos(\theta - \varphi)]} \\
 & \left\{ \frac{\alpha(\kappa - 1)}{\kappa + 1} - \frac{1 - \alpha [\cos 2\varphi + P^4 \cos 2\theta - 2P^2 \cos(\theta + \varphi)]}{\kappa + 1 [1 + P^4 - 2P^2 \cos(\theta - \varphi)]} \right\}.
 \end{aligned} \tag{13}$$

This expression completes the cases of interest in treating crack boundary value problems.

Some of the results presented in this paper have been incorporated into the general boundary condition problem required to study crack behavior via computer modeling. The method has been successfully applied to a study of hydrogen embrittlement of α -iron[15]. The usage of this type technique is particularly important in the case where nonequilibrium phenomena—such as unstable crack growth—are studied. In the case where equilibrium is reached at the end of the computation, the crack faces will be stress free as a result of relaxation and the present scheme is relevant only at the start of the computation.

Acknowledgements—The authors are grateful to J. R. Rice for helpful comments on the methodology which made the present work possible and to the U. S. Air Force Office of Scientific Research for support of this effort. Computer testing of the formalism was supported by ONR.

REFERENCES

1. R. Chang, *Int. J. Fracture Mech.* **6**, 111 (1970).
2. M. F. Kanninen and P. C. Gehlen, *Int. J. Fracture Mech.* **7**, 713 (1972).
3. J. E. Sinclair and B. R. Lawn, *Int. J. Fracture Mech.* **8**, 125 (1972).
4. P. C. Gehlen, G. T. Hahn and M. F. Kanninen, *Scripta Met.* **6**, 1087 (1972).
5. J. E. Sinclair, *J. appl. Phys.* **42**, 5361 (1971).
6. P. C. Gehlen, J. P. Hirth, R. G. Hoagland and M. F. Kanninen, *J. appl. Phys.* **43**, 3921 (1972).
7. P. C. Gehlen, R. G. Hoagland and J. P. Hirth, submitted for publication (1973).
8. R. G. Hoagland, Ph.D. Thesis, Ohio State University, Columbus, Ohio (1973).
9. J. P. Hirth, *Scripta Met.* **6**, 535 (1972).
10. C. Atkinson and D. L. Clements, *Acta Met.* **21**, 55 (1973).
11. J. R. Rice, *Fracture*, Vol. II, p. 191. Academic Press, New York (1968).
12. N. I. Muskhelishvili, *Some Basic Problems in the Mathematical Theory of Elasticity*. Noordhoff, Groningen (1953).
13. J. R. Rice, private communication, Brown University, Providence, R. I. (1972).
14. J. Dundurs and M. Hetenyi, *J. Appl. Mech. Trans ASME* **83**, 103 (1961); **84**, 362 (1962).
15. A. J. Markworth, M. F. Kanninen and P. C. Gehlen, Presented at *Int. Conf. of Stress Corrosion Cracking and Hydrogen Embrittlement of Iron Base Alloys*, Unieux-Firminy, France (12-16 June 1973).

Абстракт — Обсуждается полезность полей линейных усилий в моделировании вычислительной машины для дефектов сетки. Указывается, что эти поля дают приспособленный метод для введения реальных универсальных граничных условий для моделированных атомных кристаллитов. Даются надлежащие упругие поля для ряда линейных усилий, лежащих параллельно к вершине плоской трещины.